A HUMAN IDENTIFICATION METHOD USING IRIS FEATURE VECTOR GENERATION BASED ON HAAR WAVELET TRANSFORM AND DISCRETE COSINE TRANSFORM

ER. SALONI CHOPRA AND DR. BALRAJ SINGH SIDHU
Electronics and Communication Engineering Department,
Giani Zail Singh Punjab Technical University Campus, Bathinda, India
salonichopra06@yahoo.com and erbalrajsidhu@rediffmail.com

ABSTRACT: Though a lot of research had been done in the field of Iris recognition based automated authentication systems, still there is always a scope of improvement. This paper presented an efficient Iris recognition algorithm in which two methods have been implemented for extracting and decomposing the feature vector of the Iris pattern. Performance of Discrete Cosine Transform and different levels of decomposition of Haar Wavelet Transform have been analyzed and compared. UBIRIS ver.1 database have been used for performance evaluation of the algorithm.

KEYWORDS: Iris recognition, Multi level decomposition, Discrete Cosine Transform, Matching.

INTRODUCTION

Iris Recognition

Increasing demand for access control to the confidential areas gave birth to automated person identification. Biometrics authentication systems are most promising individual identification systems. Iris recognition is one of the challenging and most important research topic in the field of biometrics. Properties of Iris like stability, uniqueness and many more, make it efficient for person identification. Unique features of the Iris pattern like rings, crypts, cilia, connective tissues etc are taken into consideration for identification of an individual. Iris recognition is the most accurate with minimum error rate, non-contacting biometric authentication system among other biometric systems which uses face, finger print, voice, signature and so on, as one's identity.

Iris recognition has been divided into four phases: to locate the Iris boundaries in the eye image; Localization, converting the localized Iris portion into fixed dimensions; Normalization, extracting the unique features of the Iris; Feature extraction, comparing the extracted Iris template with the stored templates. If the user template gets a match, the person is identified and the person remains unidentified in case so no match. Two types of matching can be executed: one-to-many and one-to-one. In one-to-many matching, the user template is compared with many known templates that are stored in the database. This is termed as identification. Whereas, in one-to-one matching, comparison of the user template is done only with one known template stored in the database. One-to-one matching is referred to as verification. Block diagram of Iris recognition system is shown in Fig. 1.

Related Research

Though the Iris recognition prototype had been developed earlier, but Daugman was the first to give a working algorithm for automated person identification using Iris recognition, in early 1990s

Mc-GrawHill Education
GRENZE ID: 02.PEIE.2015.6.504

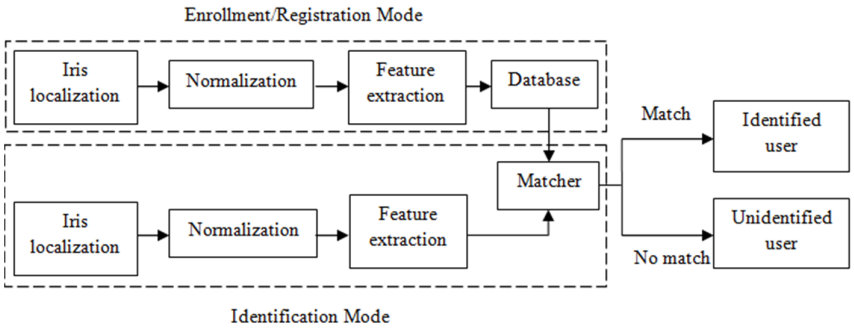

Figure 1. Block diagram of Iris recognition system

and got US Patent [2] for the proposed algorithm. Wildes [1] algorithm was the second Iris recognition algorithm to get US Patent.

Daugman's algorithm [3] was based on Integro differential operator for localizing the Iris in the eye image. Other segmentation methods include Wilde's [1] Canny edge detection [15] and Hough transform. Parabolic hough transform was used for detecting the eyelids. Boles *et al.*'s algorithm [4] includes edge detection and active contour method for locating Iris and pupil in the eye image. Lili Hsieh *et al.* [17] implemented Extended-Minima Morphology operator in order to locate the Iris. K-means clustering has been used by Liu Jin *et al.* [18].

Daugman's Rubber sheet model [3] is the most popular algorithm for normalization. Boles *et al.'s* algorithm [4] gives constant diameter of the images. Iris registration had been introduced by Wildes [1]. Polar coordinate transform has been used by Lin and Lu [16] for normalizing the segmented Iris image.

For feature extraction, Daugman [3] implemented 2-D Gabor wavelet. Zero crossing representation of 1-D wavelets was used by Boles *et al.* [4]. Wildes [1] applied Laplacian of pyramids for extracting the unique Iris features. 1-D Morlet wavelet transform was used by Lin and Lu [16]. Lim *et al.* [6] implemented Haar wavelet transform for feature extraction. 1-D Log – Gabor Wavelet has been implemented by Zhou and Sun [19]. Principle Component Analysis (PCA), subpattern based PCA, modular PCA has been used by Eskandari and Toygar [20] for recognizing the occluded Iris images.

Template matching was carried out by computing Hamming distance between the two templates by Daugman [3]. Boles *et al.* [4] performed matching by two dissimilarity functions. Wildes [1] used normalized correlation for matching purpose. Lim *et al.* [6] trained neural network for the same.

Overview of Proposed Algorithm

In the proposed algorithm, localization has been carried out by Canny edge detection and Hough transform. After the Iris boundaries are localized, fixed sized images of rectangular shape with '900×101' dimensions has been obtained with the help of Daugman's rubber sheet model by converting the Cartesian coordinates into polar coordinates. Unique features of the normalized Iris portion were extracted using 2-D Haar wavelet transform (HWT) and 2-D Discrete Cosine

Transform (DCT). With these, Iris images were decomposed and dimensions were reduced. The so formed Iris feature vectors/ binary codes/ templates were stored in the database. Performance of the algorithm has been evaluated for different levels of decomposition of HWT and DCT and hence their performance has been compared. For comparing the user feature vector with the stored feature vectors, Hamming distance (HD) has been computed between the feature vectors. A threshold (Th.) value is set. If the HD between the two templates is below the Th. value, the person is a registered person. If the computed HD between the two templates is more than the Th., the individual is an unregistered user.

Iris Image Database

Iris images for evaluation of proposed algorithm have been taken from UBIRIS v.1 database provided by SOCIA lab; Soft Computing and Image Analysis, Computer Science Engineering Department, University of Beira Interior, Covilhã Portugal [12]. UBIRIS v.1 comprises of 1877 eye images taken from 241 different subjects during 2004. These eye images were captured in two different sessions. During session 1, noise factors were reduced up to some extent and images of session 2 incorporate noises factors.

This paper has been represented in four sections. Section 1 covers the introduction to Iris recognition system, work done by various researchers, overview of the proposed Iris recognition algorithm and brief introduction to the eye image database used in the proposed work. Detailed proposed methodology is given in section II. Section III gives the result analysis and discussion of the proposed algorithm. Lastly it is concluded in section IV.

MATERIAL AND METHOD

Proposed algorithm has been implemented on MATLAB R2012a using a system with an Intel Pentium Dual 2.00 GHz Processor and 3.00Gbs RAM. Detailed explanation of the system is as follows:

Iris Boundary Localization

As mentioned in section I, localization is the process of locating the position of Iris in the eye image. In proposed algorithm canny edge detection [15], [7] and circular Hough transform [7] has been implemented to localize the inner and outer Iris boundaries. Canny edge detection gives an edge map. The process of obtaining the edge map involves four steps that are discussed as follows:
Step 1. Gaussian Filtering: Gaussian filter is first applied to the input eye image to obtain a smoothened image. It suppresses the high frequency signals in the image by performing convolution between the Gaussian function of a specified standard deviation 'σ' and the input image [7]. Gaussian filter minimizes the difference between the intensity levels of all the pixels, thus generating a blur image [8]. Smoothened blur image is thus obtained. Fig. 2 shows the original image and image after application of Gaussian filter.

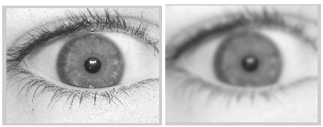

a) b)

Figure 2. a) Original image b) Result of Gaussian filter

Step 2. Gradient Operator: First order derivatives of every pixel of the smoothened image are then obtained, which are used for getting the gradient magnitude and gradient orientation. This is done by applying gradient operator to on the softened image. Equation (1) and (2) gives the gradient magnitude and orientation respectively.

$$\text{Gradient magnitude} = \sqrt{(p_x^2 + p_y^2)} \quad (1)$$

$$\text{Tan}\,\theta = p_y / p_x \quad (2)$$

In (1), 'p_x' and 'p_y' are the first order derivatives of pixels of smoothened image. 'θ' denotes the gradient orientation. 'p_x' and 'p_y' gives the rate of change of pixel intensity values of rows and columns respectively [8]. Combined change is depicted by gradient magnitude.

To enhance the image quality, gamma correction has been implemented after the application of gradient operator. Output image after gamma correction is shown in Fig. 3.

Step 3. Non maximum suppression: Output of gradient operator contains wide ridges across the local maxima [7]. These blur edges are required to be sharpened which is done by implementing non maximum suppression. A pixel intensity value is selected as local maxima. All the pixels in the current neighborhood window, that have intensity values lower than the local maxima are set as zero and others are kept unchanged. Pixels except local maxima are discarded and only local maxima are preserved and a sharp edge image is obtained. Results of non maximum suppression are shown in Fig. 4.

Figure 3. Result after gamma correction

Figure 4. Output after non maximum suppression

Step 4. Thresholding: After the non maximum suppression, wide ridges of edges were converted to sharp edges. But this sharp edge image contains some false edges along with the true edge points and these unwanted (false) edges have to be discarded. This can be achieved by thresholding the image. [7] This removes or discards all those edge points that are weaker than a certain threshold value and only the edge points stronger than the threshold level are preserved. But if the threshold value is kept very large, it may discard some of the true edges along with the false edges. In case of very low threshold value, false edges act like true edges. So, hysteresis thresholding is implemented instead of single value thresholding. In hysteresis thresholding, two levels of thresholds are set: upper threshold and lower threshold. Edge points stronger than the upper threshold are marked as strong edges and those edges points that lie between the two threshold levels are marked as weak edges in the output image. All other edge points that are weaker than the lower threshold are discarded. Final edge map contains all the strong edges and only those weak edge points which are connected to the strong edges.

Edge map obtained by implementing canny edge detection is shown in Fig. 5.

Iris boundaries have been obtained by applying Circular Hough transform which gives the contour of Iris boundaries [5].

Figure 5. Edge map achieved after canny edge detection

Normalization

Unwrapping of the Iris region has been done using Daugman's Rubber sheet model (RSM) [3], which converts the Cartesian coordinates (x,y) of the image into Polar coordinates (r,θ) and hence giving a rectangular shaped Iris image. This results in similar dimensioned Iris images. After this, the images have been enhanced by first eliminating the Iris region occluded by eyelashes and eyelids, and then the image quality has been improved by Gaussian filter. Angular and radial resolutions in the proposed work have been taken as 900 and 150 respectively.

Feature extraction

The Iris pattern in the resultant normalized Iris image was then represented by feature values stored in a feature vector. The features from Iris images have been extracted using 2-D Haar Wavelet Transform and 2-D Discrete Cosine Transform.

Feature vector generation using 2-D HWT

2-D HWT has been applied on the normalized Iris image and the obtained coefficients of HWT stored the Iris features. The coefficients of the WT, provides the frequency information of the original image in different frequency bands. Moreover the neighborhood information is also preserved in the coefficients. Multilevel decomposition has been performed. First five levels of decomposition were implemented and results were analyzed for all the five levels. Number of features goes on decreasing and more detailed features are obtained with every next level of decomposition. Then binarization was done by setting the values less than '0' to '0' and greater than '0' to '1'. Thereafter, the feature vector (row vector) has been obtained, containing pixel value '0' or '1'.

Feature vector generation using 2-D DCT

8750 Unique Iris features have been extracted using 2-D DCT and were stored in the coefficients of 2-D DCT. The normalized image has been decomposed from '900×150' to '250×35' pixels. Then the binarization was obtained by setting the negative values to '0' and positive to '1'. Hence a row vector called the feature vector has been deduced.

These feature vectors are stored in the database and were served as the input for the next step i.e. Template matching for identification purpose.

Template Matching

For identification of an individual, the iris feature vector of the entering user is generated in the same way as discussed earlier. Then this feature vector is compared with the feature vectors stored in the database. The comparison has been done on the basis of HD calculation [3] between the two feature vectors. The hamming distance has been computed according to (3) [9].

$$\text{Hamming distance} = \frac{\text{A xor B}}{\text{total length of A}} \qquad (3)$$

RESULTS AND DISCUSSIONS

Proposed algorithm has been tested on total 400 eye images: 200 from session 1 and 200 from session 2 of UBIRIS ver. 1 database.

Iris Boundary Localization

Out of 200 eye images of session 1 of UBIRIS ver.1 database, Canny Edge detection and Circular Hough transform were able to localize Iris properly on 190 eye images i.e. 95%. Same localized Iris boundaries properly on 107 eye images, i.e. 53.5%, of session 2. Fig. 6 shows the results of the Iris boundary localization.

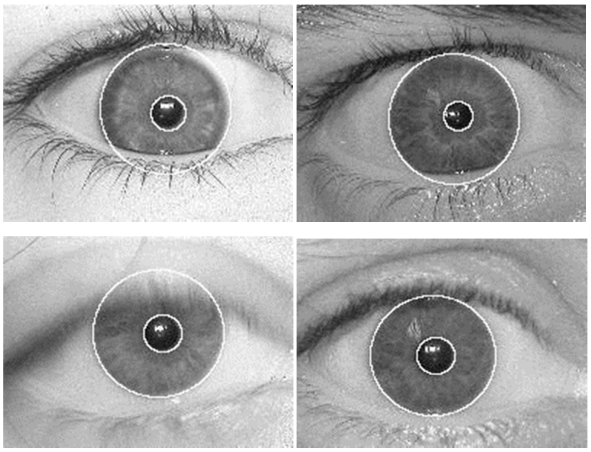

Figure 6. Eye images showing successful Iris localization

Normalization

100% success rate has been achieved on all the eye images. After normalization, dimensions of the image became '900×101' pixels from '900×150' pixels. Results of the normalization are as shown in Fig. 7.

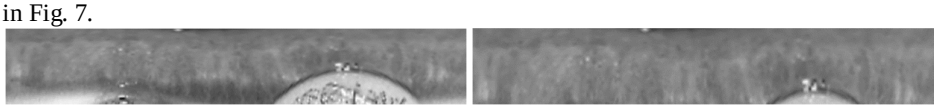

a) b)

c)

Figure 7. a) Result after Daugman's RSM, b) Result after elimination, c) Result after Gaussian filtering

Feature Extraction and Template Matching

HD for all the possible Inter class and Intra class combinations in both the sessions (1 and 2 of UBIRIS) has been computed. Total possible Inter class combinations were 39200 each for session 1 and session 2 images. Whereas, 300 times HD was calculated for Intra class images of both the sessions. Two types of errors have been computed in order to evaluate the performance of the algorithm: False Acceptance Rate (FAR); False Rejection Rate (FRR).

Performance comparison of different levels of 2-D HWT

Results have been analyzed for first five levels of decomposition of HWT. Table I shows the performance of all the levels. It shows FAR, FRR, Correct Recognition Rate (CRR) and number of features extracted by all the five levels of decomposition of HWT.

Table 1. a)1-level decomposition b) 2-level decomposition c) 3-level decomposition d) 4-level decomposition e) 5-level decomposition

SESSION	FAR (%) (Th. = 0.465)	FRR (%) (Th. = 0.465)	CRR (%) (Th. = 0.465)	No. of features extracted
Session 1	0.10	5.33	97.285	22950
Session 2	0.22	24.67	87.445	22950

a)

SESSION	FAR (%) (Th. = 0.47)	FRR (%) (Th. = 0.47)	CRR (%) (Th. = 0.47)	No. of features extracted
Session 1	0.22	5.00	97.39	5850
Session 2	0.31	23.33	88.025	5850

b)

SESSION	FAR (%) (Th. = 0.455)	FRR (%) (Th. = 0.455)	CRR (%) (Th. = 0.455)	No. of features extracted
Session 1	0.23	4.33	97.72	1469
Session 2	0.30	23.67	88.015	1469

c)

SESSION	FAR (%) (Th. = 0.415)	FRR (%) (Th. = 0.415)	CRR (%) (Th. = 0.415)	No. of features extracted
Session 1	0.11	4.33	97.78	399
Session 2	0.21	23.00	88.39	399

d)

SESSION	FAR (%) (Th. = 0.365)	FRR (%) (Th. = 0.365)	CRR (%) (Th. = 0.365)	No. of features extracted
Session 1	0.29	2.67	98.52	116
Session 2	0.38	21.00	89.31	116

e)

As it is clear from the Table I, that the performance of 4-level decomposition in terms of FAR, FRR and CRR, is the best of all the other levels. HD distribution graph for 4-level decomposition

is as shown in Fig. 8. Graphs shows the overlapping of inter and intra class HD distribution for images of session 1 and session 2.

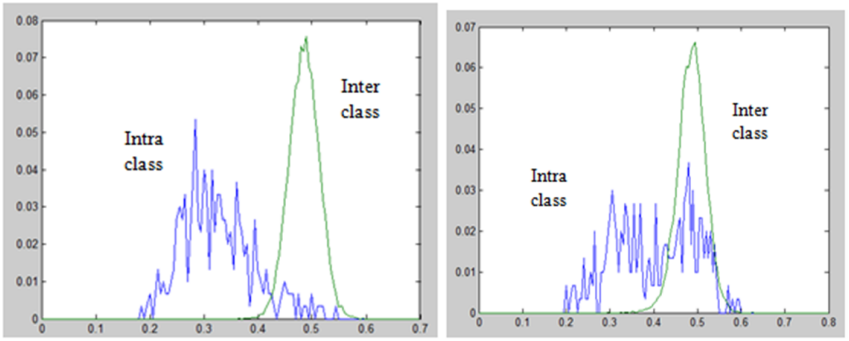

a) Session 1 b) Session 2

Fig.ure 8. Graphs showing overlapping of inter and intra class HD distribution

Performance comparison of 2-D DCT and 4-level decomposition of 2-D HWT

Table II shows the results obtained when 2-D DCT was implemented on the normalized Iris region. FAR, FRR, CRR and number of features extracted are shown in the table.

Table 2. Performance of 2-D DCT

SESSION	FAR (%) (Th.=0.5)	FRR (%) (Th.=0.5)	CRR (%) (Th.=0.5)	No. of features extracted
Session 1	0.51	8.00	95.745	8750
Session 2	0.51	8.67	95.41	8750

Fig. 9 shows the overlapping graph of inter and intra class HD distribution of images of session 1 and session 2.

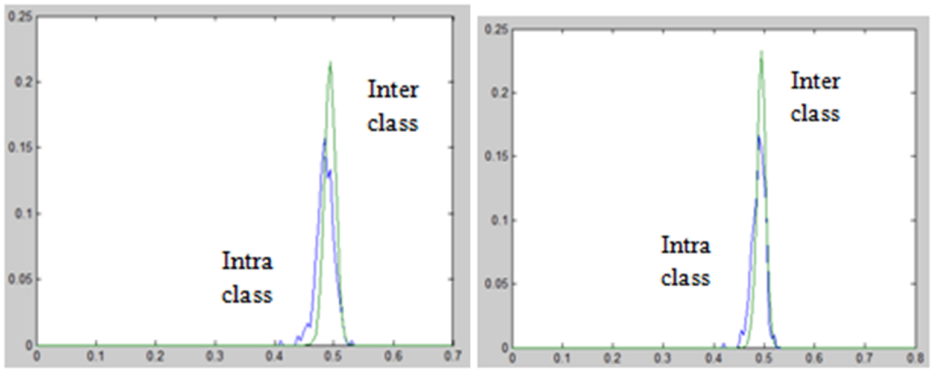

a) b)

Figure 9. Graphs showing overlapping of inter and intra class HD distribution

Table 3 shows the comparison of 2-D DCT and 4-level decomposition of 2-D HWT. It shows that the performance of 4-level decomposition of 2-D HWT is better than 2-D DCT for the images of session 1. Whereas, for session 2 images, 2-DCT shows a better performance than 4-level decomposition of 2-D HWT. On the other hand, features extracted by DCT are more so they require more storage memory.

Table 3. Comparison of both the methods

METHOD	FAR (%)		FRR (%)		CRR (%)		No. of features extracted
	Sess.1	Sess.2	Sess.1	Sess.2	Sess.1	Sess.2	
2-D DCT	0.51	0.51	8.00	8.67	95.745	95.41	8750
4-level 2-D HWT	0.11	0.21	4.33	23.0	97.78	88.36	399

CONCLUSION

An efficient method of automated Iris recognition for individual identification has been implemented in this paper. For the generation of feature vector from normalized Iris region, firstly 2-D HWT was implemented and different levels of decomposition were evaluated. With this it was concluded that the performance of 4-level decomposition of HWT is the best of all other levels. Secondly, 2-D DCT has been applied for extracting the unique features from the Iris region which gave better results than 4-level HWT on images of session 2. Whereas, on session 1 images, 4-level HWT shows better performance than DCT. It is concluded that with these methods the correct recognition rate can be increased up to 97.78% for session 1 images of UBIRIS ver.1 database and up to 95.41% for highly noisy image database (session 2).

ACKNOWLEDEGMENT

Authors would like to express their deep sense of gratitude and sincere thanks to Dr. Jyoti Saxena for their valuable guidance. Authors are also thankful to Er. Mohd. Tariq Kahn and Er. Rajveer Singh for their help and suggestions. We are thankful to Gaini Zail Singh Punjab Technical University Campus, Bathinda, India.

REFERENCES

R. P. Wildes, J. Asmuth, G. Green, S. Hsu, R. Kolcznski, J. Matey, S. McBride, "Automated, noninvasive iris recognition system and method", *U.S. Patent 5572596 A*, Nov 5, 1996.

John G. Daugman, "Biometric Personal Identification system based on Iris Analysis", *U.S. Patent 5291560 A*, March 1, 1994.

John G. Daugman, "High Confidence Visual Recognition of Person by a Test of Statistical Independence" *IEEE Transactions on Pateern Analysis and Machine Intelligence*, vol. 15, no. 11, pp. 1148-1161, 1993.

Boles and Boashash, "A Human Identification Technique using Images of the Iris and Wavelet Transform", *IEEE Transaction on Signal Processing*, vol. 46, no. 4, pp. 1185-1188, 1998.

L. Masek, "Recognition of Human Iris patterns for Biometric Identification" Technical report, School of Computer Science and Soft Engineering, The University of Western Australia, 2003.

S. Lim, K. Lee, O. Byeon, T. Kim, "Efficient Iris Recognition Through Improvement of Feature Vector and Classifier", *ETRI Journal*, vol. 23, no. 2, pp. 61-70, 2001.

R. C. Gonzalez and R. E. Woods, "*Digital Signal Processing*" 3rd Edition.

F. R. J. Lopez, C. E. P. Beain, O. E. U. Mendez, "Biometirc Iris Recognition Using Hough Transform", *18th Symposium of Image, Signal Processing and Artificial Vision*, Date of conference 11-13 Sept, pp. 1-6, 2013.

Mohd. Tariq Khan, Dr. Deepak Arora and Shashwant Shukla, "Feature Extraction through Iris Images using 1-D Gabor Filter on Different Iris Datasets", *6th International Conference on Contemporary Computing*, pp. 445-450, Aug 2013.

R. M. Farouq and R. Kumar, "Iris matching using Multi-Dimensional Artifical Neural Network", *IET Computer Vision*, pp. 178-188, 2011.

S. Chopra and Balraj S. Sidhu, "Person Identification by Iris Recognition using 2-D Reverse Biorthogonal Wavelet Transform", *International Journal of Scientific Research Engineering and Technology*, vol. 3, issue 3, pp. 707-712, 2014.

UBIRIS version 1 database, 2005, Available: http://Iris.di.ubi.pt/

G. O. Williams, "Iris Recognition Technology", *IEEE Aeroscape and Electronics Systems Magazine*, vol. 12, issue. 4, pp. 23-29, 1997.

A. K. Jain, A. Rose, S. Prabhakar, "An Introduction to Biometric Recognition", *IEEE Transactions on Circuits and Systems for Video Technology*, vol. 14, no. 1, pp. 4-20, 2004.

J. Canny, "A Computational Approach to Edge Detection", *IEEE Transaction on Pattern Analysis and Machine Intelligence*, vol. 8, no. 6, pp. 679-697, 1986.

Zhonghua Lin and Bibo Lu, "Iris Recognition Method Based on the Imaginary Coefficients of Morlet Wavelet Transform", *7th International Conference on Fuzzy Systems and Knowledge Discovery*, vol. 2, pp. 573-577, 2010.

Lili Hsieh, Wen-Shiung Chen and Tzung-Hao Li, "Personal Authentication using Human Iris Recognition based on Embedded ZerotreeWavelet Coding", *5th International Multi conference on Computing in the Global Information Technology*, pp. 99-103, 2010.

Liu Jin, FuXiao and Wang Haopeng, "Iris Image Segmentation Based on K-means Cluster" *IEEE International Conference on Intelligent Computing and Intelligent System*, vol. 3, pp. 194-198, 2010.

Steve Zhou and Junping Sun (2013) "A Novel Approach for Code Match in Iris Recognition", *12th International Conference on Computer and Information Science*, pp. 123-128.

Maryam Eskandari1 and Onsen Toygar, "Effect of Eyelid and Eyelash Occlusions on Iris Images Using Subpattern-Based Approaches", *5th International Conference on Soft Computing, Computing with Words Perceptions in System Analysis, Decision and Control*, pp. 1-4, 2009.